Polymer Journal, Vol. 24, No. 11, pp 1215—1221 (1992)

High Pressure X-Ray Measurement of *n*-Perfluoroeicosane

Shinsuke TSUBAKIHARA and Munehisa YASUNIWA

Department of Applied Physics, Faculty of Science, Fukuoka University, Jonan-ku, Fukuoka 814-01, Japan

(Received March 9, 1992)

ABSTRACT: High pressure X-ray measurement of *n*-perfluoroeicosane ($C_{20}F_{42}$) was carried out at pressures up to 500 MPa. Pressure-induced changes in the lateral packing of molecular chains and in the long period of lamellae layer structure were examined for some isothermal compressing processes. The molecular conformation and lateral packing in a high pressure phase were presumed to be the same as phase III (high pressure phase) of poly(tetrafluoroethylene). Second-order transition points, whose existence was surmised from the results of high pressure dilatometry in the preceding work, were also detected clearly. An improved phase diagram including these second-order transition points was determined.

KEY WORDS *n*-Perfluoroeicosane/$C_{20}F_{42}$/*n*-Perfluoroalkane / Poly(tetrafluoroethylene) / Oligomer / High Pressure / Phase Diagram / Second-Order Transition / X-Ray Measurement /

The phase diagram of poly(tetrafluoroethylene) (PTFE) (Figure 1) was determined,[1,2] and crystal structures in phases I—IV were clarified by X-ray measurement.[3,4] Clark and Muus[3] showed that the crystal structure and molecular conformation are, respectively, pseudohexagonal and irregular in phase I, triclinic and 13/6 helix in phase II, and hexagonal and 15/7 helix in phase IV. On the one hand, Nakafuku and Takemura[4] showed by high pressure X-ray measurement that they are orthorhombic and 2/1 helix (planar-zigzag) in phase III.

Phase transitions of PTFE oligomers (perfluoroalkanes) were also studied at atmospheric pressure.[5,6] Schwickert carried out X-ray measurement of *n*-perfluoroeicosane ($C_{20}F_{42}$) and obtained the following results.[6] $C_{20}F_{42}$ has two crystal-crystal transition points at 146 and 200 K, *i.e.*, its solid phase is divided into three phases. Its crystal structure is monoclinic in the two phases below 200 K and rhombohedral in the phase above it. In the rhombohedral phase, the molecular chains take a hexagonal lateral packing and rotate around the chain axes. Molecular conformation is 15/7 helix in the three phases, irrespective of temperature.

Recently, the authors studied phase transitions of $C_{20}F_{42}$ by high pressure differential thermal analysis (DTA) and determined its phase diagram for the first time.[7] The phase diagram is quite different from that of PTFE, as shown in Figure 2. Below about 300 MPa, a sequence of crystal–crystal transitions denoted by Tr1 and Tr2 occurs in the isobaric heating process. In the pressure region between about 300 and 400 MPa, there are two cases of crystal–crystal transition processes, one case in which a pair of Tr3 and Tr4 occurs (→Tr3→Tr4→) and the other case in which only Tr5 occurs (→Tr5→). Above about 400 MPa, only →Tr3→Tr4→occurs.

High pressure dilatometry of $C_{20}F_{42}$ was also carried out by the authors.[8] Thermodynamic parameters Δv, ΔH, and ΔS at Tr3 and Tr4 were obtained. Moreover, it is suggested from the change of compressibility that

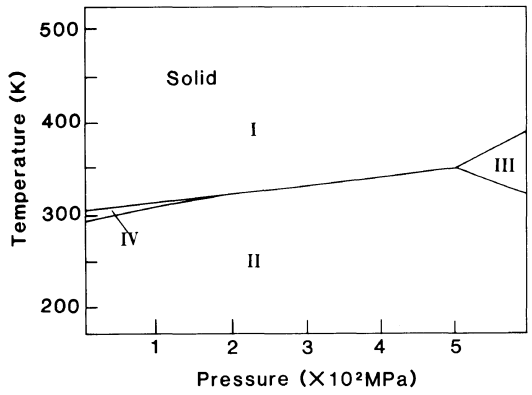

Figure 1. Phase diagram of PTFE.[2]

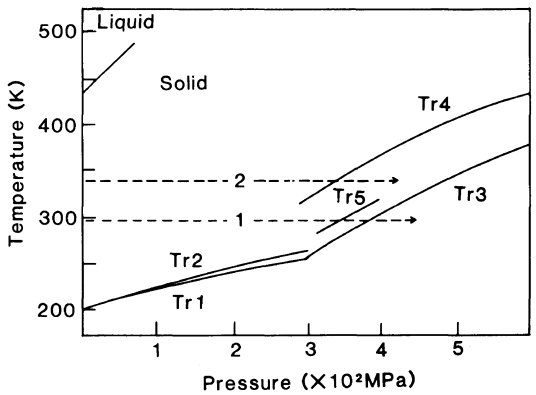

Figure 2. Phase diagram of *n*-perfluoroeicosane ($C_{20}F_{42}$), determined by high pressure DTA.[7] The full lines show crystal–crystal transitions (Tr1—Tr5) and melting. Dotted lines 1 and 2 represent the isothermal compressing processes along which the pressure-induced changes in the X-ray diffraction pattern were examined in this work.

second-order transitions, which could not be detected by high pressure DTA, occur in the pressure region below about 300 MPa.

In these our previous works, the phase transitions of $C_{20}F_{42}$ under pressure were studied from the viewpoint of thermodynamics. Therefore, detailed transition mechanisms have not yet been clarified. In this work, high pressure X-ray measurement of $C_{20}F_{42}$ was conducted to clarify the structural changes through these high pressure transitions. Pressure-induced changes in the lateral packing of molecular chains and the long period of

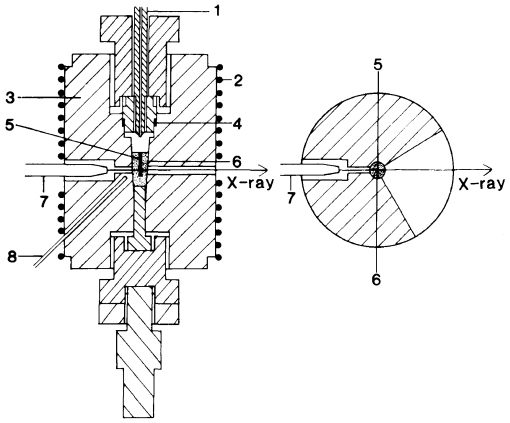

Figure 3. Schematic picture of the apparatus for high pressure X-ray measurement. 1, high pressure pipe; 2, sheathed heater; 3, high pressure vessel; 4, copper seal; 5, sample; 6, beryllium sample cell; 7, pinhole collimator; 8, sheathed Alumel-Chromel thermocouple.

lamellae layer structure were examined. In addition, second-order transition points, suggested to exist by high pressure dilatometry, were also examined in detail. Based on these results, the transition mechanisms under high pressure are discussed.

EXPERIMENTAL

Sample $C_{20}F_{42}$ was purchased from Aldrich Chemicals Co., Inc., which was the same pure sample as that used for high pressure DTA and dilatometry.

A diffraction pattern of a powder sample was recorded at atmospheric pressure and room temperature with a diffractometer using nickel-filtered Cu-$K\alpha$ radiation, and lattice constants at this point were calculated from it.

High pressure X-ray measurement was carried out at pressures up to 500 MPa using the apparatus shown in Figure 3. This apparatus is basically the same as that made by Tanaka *et al.*[9] A sample cell was made of beryllium whose absorption coefficient for X-ray radiation is small and whose reflections do not exist at the angles of main reflections

form the sample. A silicone oil (Shin-Etsu Chemicals Co., KF-96L-10CS, 10cSt) was used as the pressure transmitting fluid. Hydrostatic pressure was measured within $\pm$1MPa by a Bourdon's gauge (Heise Co., U.S.A.) connected to the high pressure apparatus. Temperature of the sample was measured with an Alumel-Chromel thermocouple placed near the sample cell. The apparatus was cooled by spraying low temperature nitrogen gas on it.

Pressure-induced changes in the X-ray diffraction pattern of a powder sample were examined for some isothermal compressing processes, including paths 1 and 2 in Figure 2. A cylindrical powder sample of 1 mm diameter was set in the beryllium cell. The sample was irradiated with a pinhole-collimated X-ray beam and its diffraction pattern detected by a scintillation counter. A Rigaku Rotaflex RU-200 (60 kV, 200 mA) was used as the X-ray generator. Because the reflection intensities were attenuated by passing through the beryllium cell, only two intense reflections could be detected clearly at atmospheric pressure. One was a reflection corresponding to the long period of lamellae layer structure in the small angle region, and the other a reflection corresponding to the lateral packing of molecular chains in the large angle region. In this work, the pressure changes of these two reflections in the small and large angle regions were examined using nickel-filtered Cu-$K\alpha$ and zirconium-filtered Mo-$K\alpha$ radiation, respectively.

RESULTS AND DISCUSSION

Figure 4 shows the diffraction powder pattern of $C_{20}F_{42}$, measured at room temperature and atmospheric pressure with a diffractometer. Reflection 1 ($2\theta=3.04°$) in the small angle region corresponds to the long period of lamellae layer structure, and the most intense reflection 2 ($2\theta=17.92°$) in the large angle region corresponds to the lateral packing of molecular chains. Schwickert showed that the

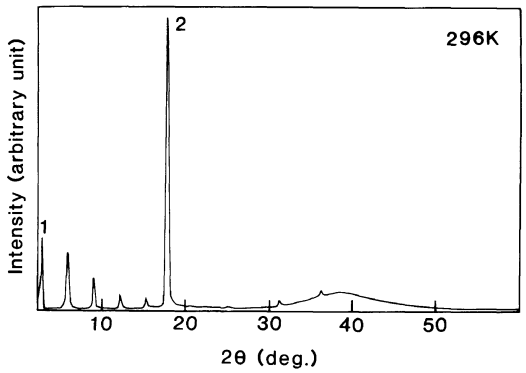

Figure 4. X-Ray diffraction pattern of $C_{20}F_{42}$, measured at room temperature (296 K). Nickel-filtered Cu-$K\alpha$ radiation was used. Reflections 1 and 2 correspond to the long period of lamellae layer structure and the lateral packing of molecular chains, respectively.

crystal structure of $C_{20}F_{42}$ is rhombohedral at this point. Lattice constants of the hexagonal unit cell adopted for this rhombohedral structure are:

$$a=b=5.71\,\text{Å},\quad c=87.15\,\text{Å},\quad \text{and}\quad \gamma=120°.$$

Reflections 1 and 2 are from the (003) and (100) lattice planes of this hexagonal lattice, respectively. In this structure, molecular chains take a hexagonal lateral packing and rotate around the chain axes.[6] The single peak of reflection 2 shows this hexagonal lateral packing of the rotating molecular chains.

Figure 5 shows the pressure-induced changes of reflection 2 in the compressing process at 296 K (path 1 in Figure 2), measured by high pressure X-ray measurement using Mo-Kα radiation. At atmospheric pressure, a single reflection corresponding to the hexagonal lateral packing of the rotating molecular chains appears. This packing is shown schematically in Figure 6a. At 177 and 343 MPa, this single reflection appears and shifts to larger angles as the pressure increases due to the contraction of intermolecular distance. On the other hand, two reflections appear instead of it at 437 MPa. This indicates that the crystal structure at this pressure is different from that at the lower

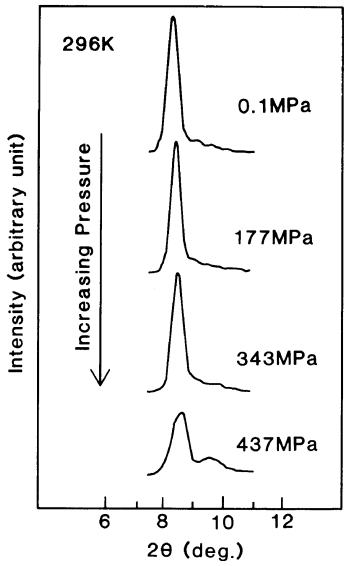

Figure 5. Pressure-induced changes of reflection 2 in the isothermal compressing process along path 1 in Figure 2 (296 K), measured with the apparatus shown in Figure 3. Zirconium-filtered Mo-$K\alpha$ radiation was used.

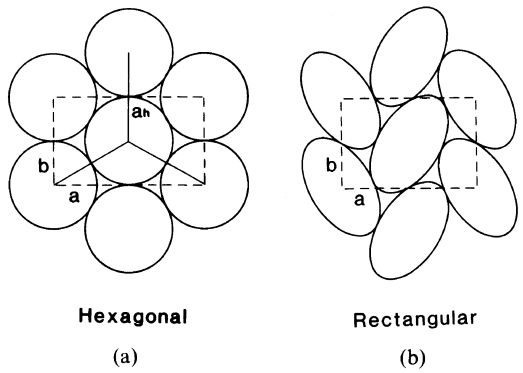

Figure 6. Lateral packing of molecular chains viewed along the chain axis. (a) Hexagonal lateral packing of rotating molecular chains represented by circles. (b) Rectangular lateral packing of 2/1 helical (planar-zigzag) molecular chains represented by ellipsoids (herringbone type). Dotted rectangles in both pictures give planar lattices with a and b lattice constants.

pressures, which gives the single reflection. The molecular conformation and lateral packing giving the two reflections are deduced as follows.

It is well known that the majority of n-alkanes, *i.e.*, polyethylene oligomers have the same molecular conformation and lateral packing as polyethylene. Moreover, $C_{20}F_{42}$ takes 15/7 helical conformation and hexagonal lateral packing at atmospheric pressure, the same as PTFE. As shown in these examples, oligomers tend to take the same molecular conformation and packing in the crystal as the polymer composed of the same repeating units under similar conditions. If this holds for the case of $C_{20}F_{42}$ under high pressure, it is possible that it takes 2/1 helical conformation and rectangular lateral packing as shown in Figure 6b under high pressure, the same as phase III of PTFE (Figure 1).[4] Because of the lack of reflections from $C_{20}F_{42}$, it is difficult to establish the relation between the crystal structure of $C_{20}F_{42}$ at 437 MPa and that of PTFE in phase III by a comparison of their complete X-ray diffraction patterns. However, because both structures give the same number and profile of reflections corresponding to the lateral packing, it is presumed that they take the same molecular conformation and lateral packing. To confirm this, it is necessary to raise the sensitivity of the X-ray apparatus and record an X-ray diffraction pattern of $C_{20}F_{42}$ in more detail under high pressure.

Figure 7 shows pressure-induced changes in lattice spacing d of reflection 2, measured along path 1 in Figure 2. At crystal-crystal transition Tr3 (380 MPa), the single line of d separates into two. This indicates that $C_{20}F_{42}$ takes the hexagonal and, presumably, rectangular lateral packings on the high and low temperature sides of the Tr3 transition line, respectively. In the rectangular one, molecular chains do not rotate around the chain axes. Therefore, the rotational motion of the molecular chains is activated at Tr3 in the isobaric heating process if the presumed packing is correct. This was shown by high pressure dilatometry carried out for $C_{20}F_{42}$ in the preceding work.[8]

The line of lattice spacing d bends at about 200 and 300 MPa, as shown by the arrows. This indicates that second order transitions occur at these pressures. By high pressure dilatom-

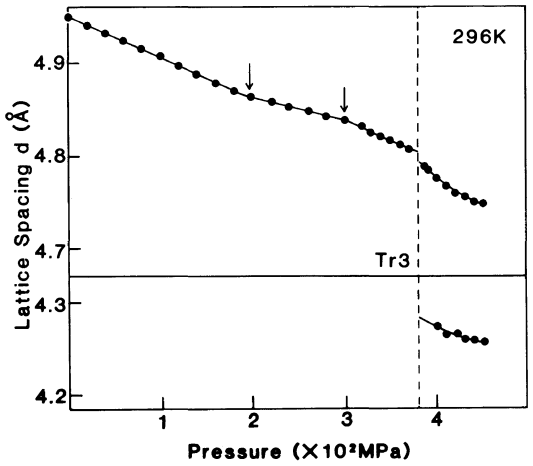

Figure 7. Pressure-induced changes in lattice spacing d of reflection 2 along path 1 in Figure 2 (296 K). Dotted line represents the pressure (380 MPa) corresponding to the intersection of Tr3 transition line and path 1 in Figure 2, *i.e.*, the pressure at which Tr3 is expected to occur in this isothermal compressing process.

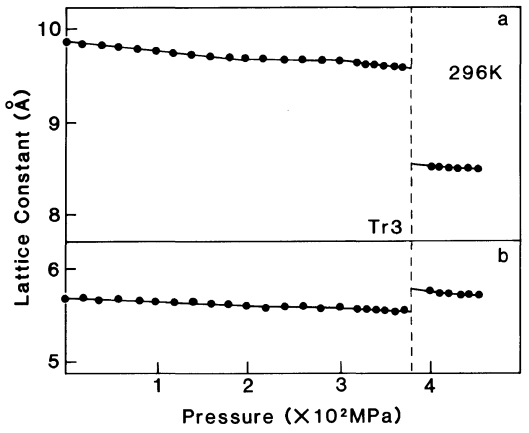

Figure 8. Pressure-induced changes in rectangular lattice constants a and b (Figure 6) along path 1 in Figure 2 (296 K). The values were calculated from the data in Figure 7.

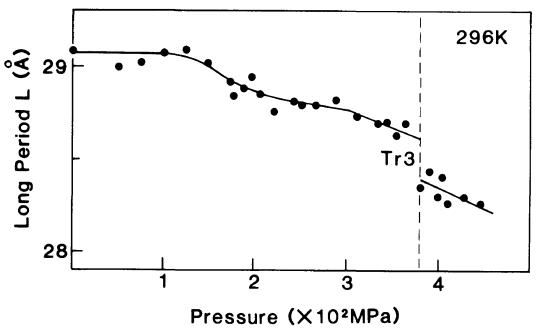

Figure 9. Pressure-induced changes in long period L, measured along path 1 in Figure 2 (296 K). This long period was obtained from the lattice spacing of reflection 1 in Figure 4.

etry, it was also shown that two second-order transitions occur at about 200 and 250 MPa in the same compressing process.[8] Lower pressure transition points from X-ray measurement and dilatometry coincide. However, the results diverge at higher pressures. The used dilatometry apparatus is not sensitive enough to determine definitively the second-order transition point. This is thought to be the cause of the difference between the results of the two measurements.

The transition point of Tr5 is found at 344 MPa on the dotted line of path 1 in Figure 2. However, there is no change at this pressure in Figure 7. That is, Tr5 does not occur in this compressing process. This was also confirmed by high pressure dilatometry.[8]

Figure 8 shows pressure-induced changes in rectangular lattice constants a and b (Figure 6) along path 1. These data were calculated from lattice spacing d in Figure 7. Both a and b decrease continuously with pressure except for the discontinuous change at Tr3. At this pressure, a decreases and b increases. It is noted that the values of a, b, and a/b (*ca.* 1.49) in the high pressure phase above Tr3, calculated based on the assumption that $C_{20}F_{42}$ takes the same rectangular lattice as phase III of PTFE, are close to the values in phase III, *i.e.*, 8.73 Å, 5.69 Å, and 1.53,[4] respectively.

Figure 9 shows pressure-induced changes in long period L, measured at 296 K along path 1. Because the data scatter appreciably, it is difficult to draw a definitive curve giving the pressure-induced changes in L. Therefore, the curve supposed to be most probable by the authors was drawn. According to the curve, the value of L decreases appreciably in the

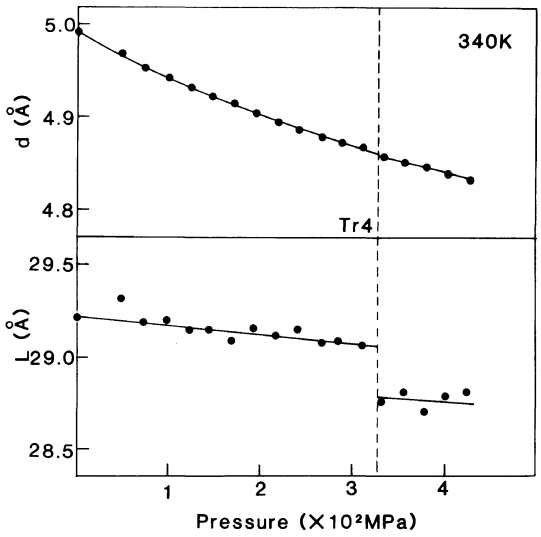

Figure 10. Pressure-induced changes in lattice spacing d and long period L, measured along path 2 in Figure 2 (340 K). Dotted line represents the pressure (330 MPa) at which transition Tr4 is expected to occur in this isothermal compressing process.

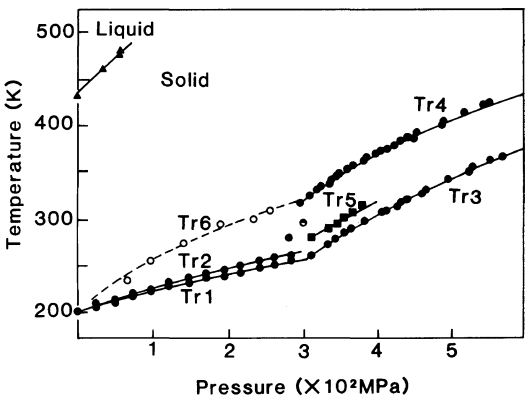

Figure 11. Phase diagram of $C_{20}F_{42}$, including second-order transition points. ● (Tr1—Tr4) and ■ (Tr5) represent first-order (crystal–crystal) transition points, and ▲ represents melting points, obtained by high pressure DTA in the isobaric heating processes (heating rate, 5 K min^{-1}). ○ (Tr6) and ◓ represent second-order transition points obtained by high pressure X-ray measurement in the isothermal compressing processes.

pressure region between 150 and 200 MPa. This change may occur through the second-order transition identified at about 200 MPa in Figure 7. Moreover, L decreases discontinuously at Tr3. Two factors, tilting of molecular chains from the direction perpendicular to their layer surface and decrease of the thickness of lamellar interfacial layer due to the depression of dynamic disorder,[10] are considered to be responsible for the decrease of long period L, occurring in the pressure region of 150—200 MPa and at Tr3.

Figure 10 shows pressure-induced changes in lattice spacing d and long period L at 340 K, measured along path 2 in Figure 2. Both d and L decrease discontinuously at 330 MPa, corresponding to Tr4. In this figure, there is no bending point such as is found in Figure 7. That is, no second-order transition occurs along path 2.

The phase diagram of $C_{20}F_{42}$, including the second-order transition points measured in some isothermal compressing processes, is shown in Figure 11. ● (Tr1—Tr4) and ■ (Tr5) represent first-order (crystal-crystal) transition points, and ▲ represents melting points, obtained previously by high pressure DTA in isobaric heating processes.[7] ○ (Tr6) and ◓ represent second-order transition points, obtained by high pressure X-ray measurement in this work. The second-order transition point represented by ◓ was identified only at 296 K (path 1 in Figure 2). Tr6 second-order transition line extends from Tr4 first-order one to the common transition point of Tr1 and Tr2 at atmospheric pressure. That is, there is a solid phase bounded by Tr2 and Tr6 transition lines below about 300 MPa.

As shown in this figure, the phase diagram of $C_{20}F_{42}$ is very complicated. In this work, structural changes occurring at the high pressure transitions were partly clarified. To clarify the transition mechanisms completely, further study with a variety of experimental techniques is desired.

Acknowledgments. We thank Prof. K. Matsushige and Dr. T. Horiuchi of Kyushu University for advice regarding the high

pressure X-ray apparatus and for useful discussions.

REFERENCES

1. C. E. Weir, *J. Res. Natl. Bur. Stand.*, **50**, 95 (1953).
2. S. Hirakawa and T. Takemura, *Jpn. J. Appl. Phys.*, **8**, 635 (1969).
3. E. S. Clark and L. T. Muus, *Z. Krist.*, **117**, 119 (1962).
4. C. Nakafuku and T. Takemura, *Jpn. J. Appl. Phys.*, **14**, 599 (1975).
5. H. W. Starkweather, Jr., *Macromolecules*, **19**, 1131 (1986).
6. H. Schwickert, G. Strobl, and M. Kimmig, *J. Chem. Phys.*, **95**, 2800 (1991).
7. S. Tsubakihara and M. Yasuniwa, *Polym. J.*, **24**, 421 (1992).
8. S. Tsubakihara, K. Higashi, S. Taki, K. Matsushige, and M. Yasuniwa, *Polym. J.*, in press.
9. H. Tanaka, K. Takayama, T. Okamoto, and T. Takemura, *Polym. J.*, **14**, 719 (1982).
10. G. Strobl, B. Ewen, E. W. Fischer, and W. Piesczek, *J. Chem. Phys.*, **61**, 5257 (1974).